ELSEVIER

Materials Science and Engineering A 456 (2007) 350–357

MATERIALS SCIENCE & ENGINEERING A

www.elsevier.com/locate/msea

Influence of heat treatment on degradation behavior of bio-degradable die-cast AZ63 magnesium alloy in simulated body fluid

Chenglong Liu [a], Yunchang Xin [a,b], Guoyi Tang [b], Paul K. Chu [a,*]

[a] *Department of Physics and Materials Science, City University of Hong Kong, Tat Chee Avenue, Kowloon, Hong Kong*
[b] *Tsinghua University, Shenzhen Graduate School, Shenzhen 518055, China*

Received 4 September 2006; received in revised form 25 November 2006; accepted 7 December 2006

Abstract

The effects of hybrid aging and solution treatments on the degradation of bio-degradable die-cast AZ63 magnesium alloy in 37 ± 1 °C Tyrode's simulated body fluid have been investigated. The heat treatment is observed to alter the microstructure of the alloy. The amount of β-$Mg_{17}Al_2$ precipitates is larger and their distribution is more homogeneous. The homogeneous microstructure enhances the corrosion resistance of the alloy and the best corrosion rate achieved on the aged sample is approximately 1/2 of that of the untreated alloy. The corrosion mechanism of the aged alloy is dominated by filiform and pitting corrosion. Better understanding and control of surface corrosion will expedite the use of Mg alloys in biomedical implants.

PACS: 47.54.Jk; 81.40.Cd; 81.65.Kn

Keywords: AZ63 magnesium alloy; Aging; Corrosion resistance; Degradation; Simulated body fluid

1. Introduction

Traditional biomedical metal materials such as stainless steels and Ti and Ti alloys have played an essential role in load-bearing implants for the repair or replacement of diseased or damaged bone tissues. Durable implants represent a foreign body and bear the risk of local inflammation. Furthermore, the stress-shielding effect may obstruct the stabilization of the bone tissues that need mechanical loads to obtain and maintain their rigidity [1]. Degradable biocompatible implants, which dissolve in a biological environment, constitute an appropriate solution. Unfortunately, currently used absorbable materials such as poly-lactides have unsatisfactory mechanical properties. In comparison, magnesium-based alloys possess a more attractive combination of desirable properties including low density, good elastic modulus, and compressive yield strength closer to those of natural bones, in addition to their high strength to weight ratio [2]. Magnesium also has good biocompatibility and is thus a potential candidate in bone implants. However, the major drawback of magnesium alloys is that they tend to corrode very quickly in the physiological pH (7.4–7.6) environment thereby losing their mechanical integrity before the tissues have sufficient time to heal. Furthermore, rapid production of hydrogen gas during the corrosion process may not be tolerated by the host tissues [3]. Nevertheless, the use of magnesium alloys as bio-degradable implants is still promising, but their corrosion resistance must be enhanced [4,5].

New casting techniques can produce magnesium alloys with a minimal amount of impurities and help to control in vivo corrosion. However, the corrosion process does not depend on the elemental composition and processing history only [4]. Effective means to mitigate corrosion include the application of a surface coating in order to separate the metal surface from its surroundings or incorporation of corrosion inhibiting chemicals. Different surface modification techniques such as electrochemical plating, conversion coatings, anodization, gas-phase deposition, laser surface alloying/cladding, and organic coatings have been proposed for this purpose [6]. To be effective, the coating must be uniform, sticking, pore-free, and self-healing. Unfortunately, magnesium alloys have high chemical reactivity, and once they come in contact with air or water, an oxide/hydroxide layer forms readily on the surface which can

* Corresponding author. Tel.: +852 27887724; fax: +852 27889549.
E-mail address: paul.chu@cityu.edu.hk (P.K. Chu).

0921-5093/$ – see front matter © 2006 Elsevier B.V. All rights reserved.
doi:10.1016/j.msea.2006.12.020

Table 1
Heat treatment parameters

	#1	#2	#3	#4
Solution treatment	Untreated	413 °C, 24 h	413 °C, 24 h	413 °C, 24 h
Aged treatment	Untreated	216 °C, 1 h	216 °C, 5.5 h	216 °C, 12 h

have a detrimental effect on adhesion and uniformity. There is a close relationship between the coating and magnesium alloy substrate. In fact, chemical heterogeneity caused by crystallization, precipitation, and segregation during the casting process can have a negative impact on the surface corrosion resistance.

Heat treatments can cause micro-structural changes and redistribution of metal elements. A homogeneous structure can be obtained by a hybrid solution and aging process [7]. Wang et al. have studied the changes in the microstructures of AZ91D magnesium alloy during T4 or T6 treatments [7]. A solution treatment at 413 °C causes micro-structural evolution involving four processes: dissolution of the β phase, formation of a fine-grain structure, morphological change of the globules into a traditional grain shape, and grain coarsening. During aging at 216 °C, discrete precipitates are preferentially initiated at some of the grain boundaries and then interconnected precipitates emerge inside the grains with accelerated age-hardening kinetics. These micro-structural changes can affect selected properties of the magnesium alloys. Zhang et al. have found that a solution treatment decreases the amount of second-phase particles inside the grains and weakens strong pinning on dislocations. The T4 treatment (solution) improves the ductility substantially but reduces strength, whereas the T6 (solution plus aging) process increases the ultimate tensile strength but compromises the yield strength and ductility [8].

It has been reported that the secondary phase has an effect on the corrosion resistance of aluminum-containing magnesium alloys [9–12]. The β phase plays dual roles that depend on the amount and distribution of this phase. A fine and homogeneous phase appears to be a better anti-corrosion barrier. Otherwise, the presence of the β phase in the alloys could deteriorate the corrosion performance as it can act as an effective galvanic cathode. The beneficial effect of the β phase on the corrosion properties may be enhanced by grain refinement. Song et al. [11] have pointed out that moderate temperature (160 °C) aging of die-cast AZ91D changes the corrosion resistance in 5 wt.%NaCl saturated with $Mg(OH)_2$. Aging at temperatures up to 230 °C for 36 h has only a slight effect on the corrosion resistance, but a temperature above 230 °C significantly reduces the corrosion resistance of die-cast AZ91 under salt spraying [13]. The influence of the hybrid solution and aging treatment on the corrosion resistance of biomedical Mg alloys in a simulated body environment has hitherto been seldom probed. From a practical point of view, it is important to know the effects of the suitable heat treatment on the degradation rate in an in vitro environment. Better understanding of the process and mechanism can improve the degradation rate of magnesium alloys in a biological medium thereby expediting the acceptance and use of the bio-degradable materials in biomedical implants.

2. Experimental details

The composition of the die-cast AZ63 alloy used in this study is as follows: Mg–5.9 wt.%Al–3.5 wt.%Zn–0.18 wt.% Mn–0.04 wt.%Si–0.004 wt.%Fe–0.003 wt.%Ni. The materials that were purchased from YiHo Corporation, Shenzhen, China were produced by die-casting. Circular disks 2 mm thick were cut from the alloy rod with a diameter of 10 mm. Samples with dimensions of 10 mm × 10 mm × 2 mm were used in the in vitro degradation tests.

2.1. Heat treatment

The AZ63 samples were subjected to heat treatments described in Table 1 [7]. The solution treatment was carried out at 413 °C for 24 h (T_4) in air with the sample surface protected by carbon powders. The samples were cooled in air and then aged for different periods of time. The micro-structural evolution during heat treatment was examined by an Olympus optical microscope (OM). The specimens for OM were prepared by a standard technique of grinding with SiC waterproof abrasive paper, polishing with an Al_3O_2 suspension solution, and etching in a 2% nital solution.

2.2. In vitro corrosion measurements

All the corrosion tests were carried out at 37 ± 1 °C in Tyrode's simulated body fluid (SBF) with the following composition (mmol/l)—NaCl: 100.0, KCl: 10.0, KH_2PO_4: 1.2, $MgSO_4$: 5.0, glucose: 20.0, taurine: 10.0 and MOPS: 10.0. The solution was maintained at the normal physiological pH at 7.2. A 0.9 wt.% physiological saline was also used.

2.2.1. In situ corrosion measurement

The specimens were etched in a 2% nital solution initially to unravel their microstructures. They were then immersed horizontally about 1 mm below the surface of the test solution. An optical microscope was mounted above the solution to monitor the corrosion process with time. Afterwards, the specimens were quickly washed with alcohol, dried, and examined under an optical microscope again.

2.2.2. Immersion test

The immersion test was carried out at 37 ± 1 °C. Each sample was ground by #2400 waterproof abrasive paper and then ultrasonically cleaned in alcohol for 5 min before testing. The Mg ion concentration of each sample after different immersion time was determined thrice using a SHIMADZU atomic absorption flame emission spectrophotometer (AA6501S) at an excitation wavelength of 285.2 nm.

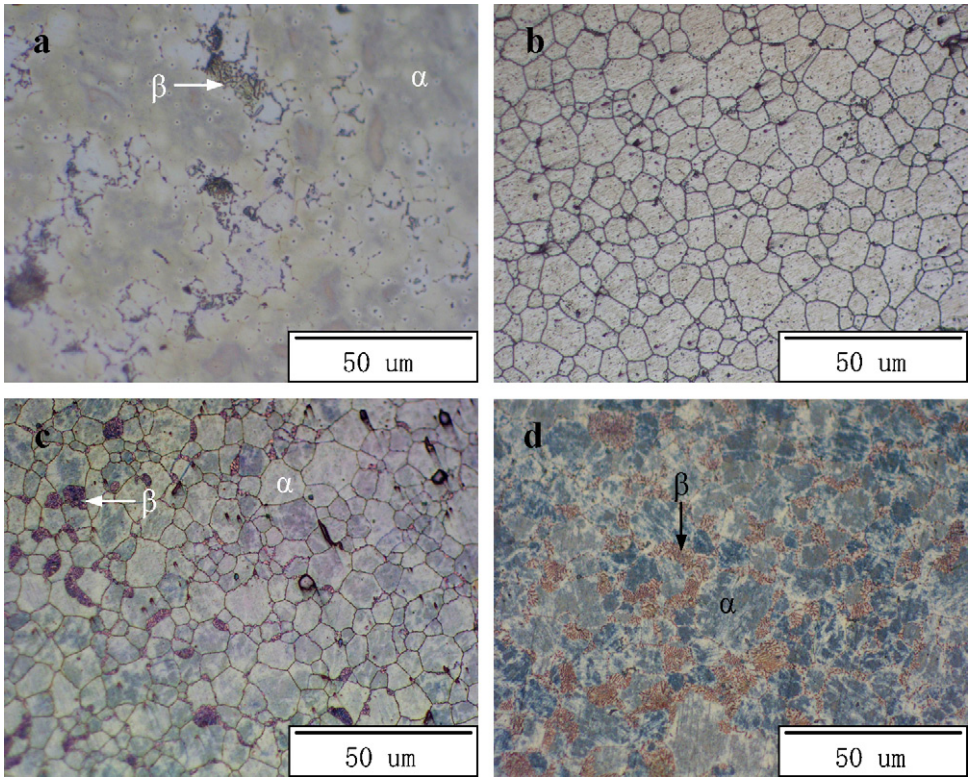

Fig. 1. Typical optical microstructure of the die-cast AZ63 alloy solution at 413 °C for 24 h followed by another aging step at 216 °C for different periods of time: (a) as-received sample, (b) 1 h, (c) 5.5 h, and (d) 12 h.

2.2.3. Corrosion rate measurement

After the immersion tests, the corroded specimens were removed from the solution, cleaned with distilled water, and dried. They were then immersed in chromate acid (200 g/l CrO_3 + 10 g/l $AgNO_3$) for 5–10 min to remove the corrosion products. Afterwards, the specimens were washed with distilled water and dried again. The dried specimens were weighed and the corrosion rate was calculated as follows:

$$\mathrm{CR} = \frac{W}{At}, \tag{1}$$

where CR is the corrosion rate, W the weight loss, A the original surface area exposed to the test solution, and t is the exposure time [5].

2.2.4. Free corrosion potential evaluation

The free corrosion potential was measured using an M273 EG&G potentiostat. The experimental setup consisted of a conventional three-electrode cell comprising a working electrode, saturated calomel electrode (SCE), and pure carbon stick as the counter electrode. The specimens were prepared by connecting a copper plate to one side of the sample covered by cold setting resin. The opposite surface of the specimen was exposed to the solution. The exposed area was about 1 cm^2. The changes in the free corrosion potential (E_{corr}) were monitored as a function of time under open circuit conditions for approximately 4000 s.

3. Results

The typical optical micrographs of the as-received (sample 1) and heat-treated (samples 2–4) AZ63 alloys are depicted in Fig. 1. The die-cast AZ63 Mg alloy exhibits a microstructure with the primary α phase grains and β-$Mg_{17}Al_{12}$ phase dispersed heterogeneously in the matrix. Fig. 1a shows the partial continuous network of the β phase. After 1 h aging, more homogeneous microstructures are formed and the β phase dissolves in the α phase as shown in Fig. 1b. With increasing aging time (Fig. 1c), the β phase precipitates from the super-saturated α-Mg solid solution [7]. Discontinuous precipitation of the β phase is typically initiated preferentially at some of the grain boundaries, as indicated by coarse lamellar growth into the grains. After 12 h aging, the microstructure is observed to be different from that aged for 5.5 h. Both the amount and continuity of the β phase increase. Fig. 1d shows the continuous precipitation lamellae from the grain boundary into the grain and fine continuous precipitation lamellae form inside the α-Mg grains [7].

The micro-corrosion morphologies of AZ63 in Tyrode's simulated body fluid as a function of immersion time are shown in Figs. 2 and 3. Based on the optical micrograph acquired from sample 1 (untreated), intensive hydrogen evolution takes place mainly at the center of the α phase grain immediately after the sample is dipped in the test solution. In contrary, few hydrogen bubbles form on the aged sample surfaces. After 10 min exposure, heavy localized corrosion attack appears on sample 1 whereas only few localized corrosion holes can be seen on the

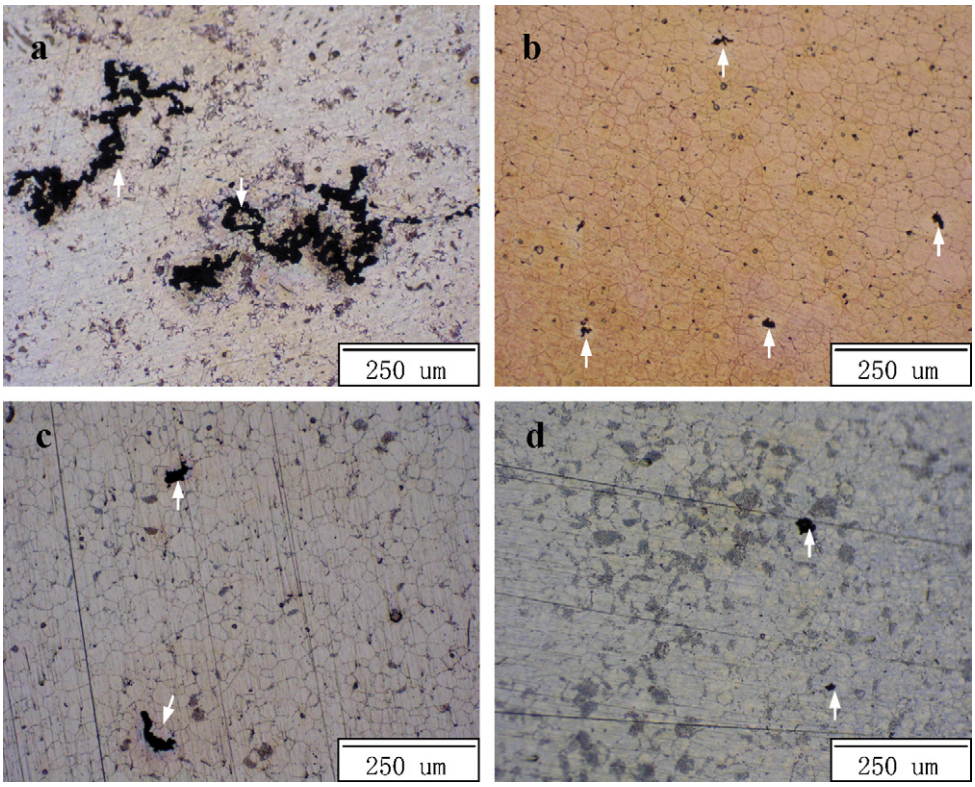

Fig. 2. Optical micrographs of the AZ63 surfaces after 10 min exposure in Tyrode's simulated body fluid for samples aged for different periods of time: (a) sample 1 (untreated), (b) 1 h, (c) 5.5 h, and (d) 12 h (corrosion holes indicated by arrows).

surfaces of the aged samples. Compared to samples 2 and 3, sample 4 suffers the slightest corrosion attack. The α phase grains are corroded but this does not affect the β phase. A similar behavior has been reported for AZ91 alloy [11]. With increasing immersion time, the developing rate and amount of hydrogen bubbles increase rapidly for sample 1 while hardly any changes can be observed on the aged samples. After 12 h immersion, sample 1 is badly corroded as manifested by abundant clusters formed by localized corrosion (Fig. 3a). Compared to the surface morphology after 10 min, the number of localized corrosion holes

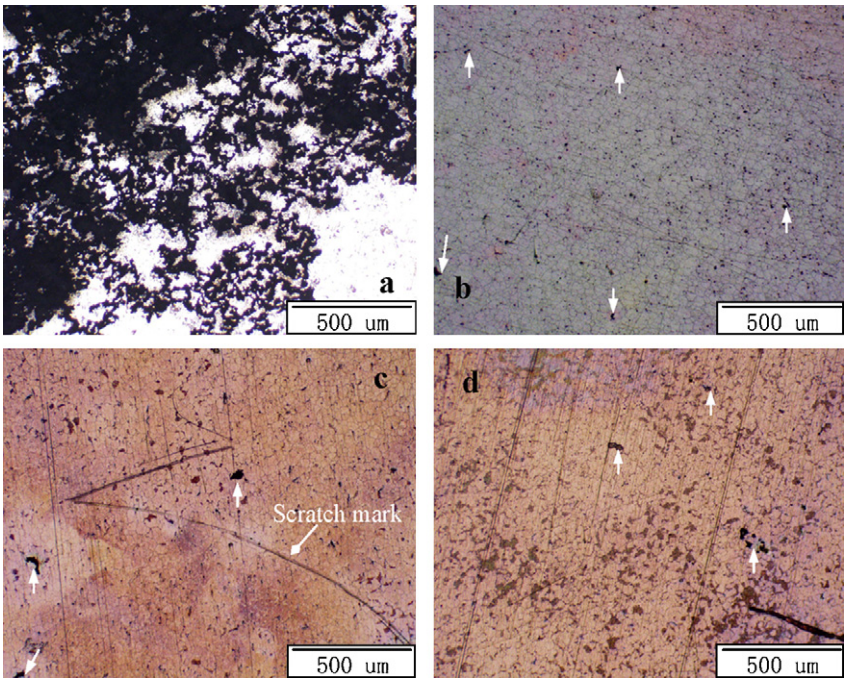

Fig. 3. Optical micrographs of the AZ63 surfaces after 12 h exposure in Tyrode's simulated body fluid for samples aged for different periods of time: (a) sample 1 (untreated), (b) 1 h, (c) 5.5 h, and (d) 12 h (corrosion holes indicated by arrows).

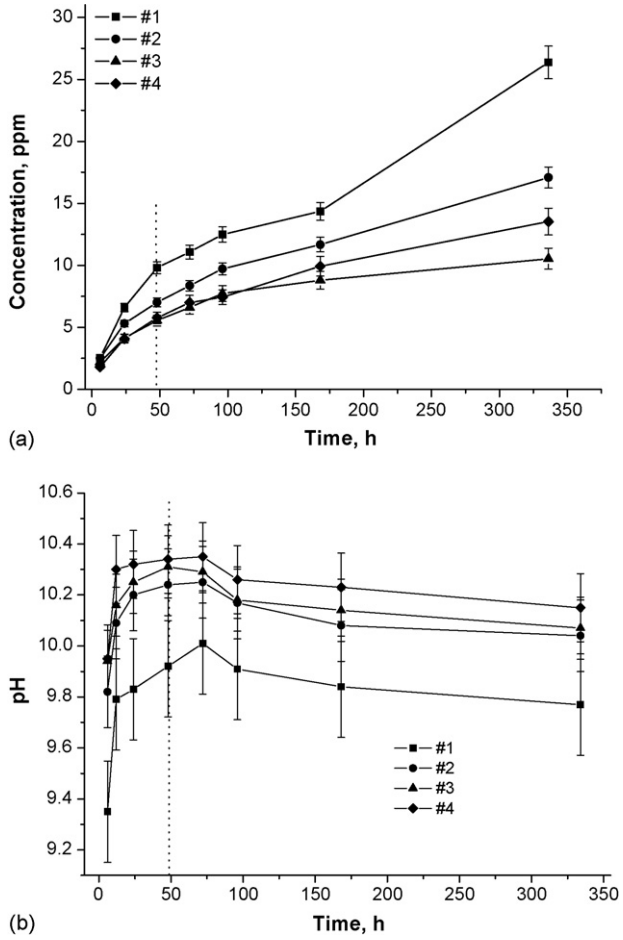

Fig. 4. Changes in of Mg ion concentration and pH as a function of immersion time: (a) Mg ion concentration; (b) pH value.

increases on the aged samples, but corrosion does not lead to breakdown of the entire sample surface. No extensive localized corrosion can be observed around the scratch mark in Fig. 3c indicating that the scratch does not affect the corrosion property significantly.

In order to investigate the effects of different heat treatments on the long-term degradation behavior, the untreated and aged AZ63 samples were immersed in 0.9 wt.% physiological saline at $37 \pm 1\,^{\circ}C$ for different periods of time. Fig. 4 shows the variation of the Mg ion concentration and pH as a function of the immersion time. It is interesting to note the relative change in the pH and magnesium dissolution rates after different exposure time. Between 6 and 48 h, both the Mg ion concentration and pH value increase quickly suggesting localized corrosion attack. After 48 h immersion, the Mg ion concentration increases more slowly but the pH of the test solution decreases suddenly at 96 h before stabilizing afterwards. The Mg ion concentration measured from sample 1 is greater than those of the aged samples at each testing time point, indicating a greater corrosion rate.

The corroded morphology was examined after 14 days immersion. The samples (1 cm^2) polished with #2400 SiC waterproof paper were submerged in the test solution. Corrosion attack on a large area is observed on samples 1 and 2, and with increasing immersion duration, it is deeper as shown in Fig. 5a and b. "Filiform" corrosion and pitting corrosion are seen on the surface of samples 3 and 4 (Fig. 5c and d) but the attack is not as severe [14].

Dissolution in body fluids is the major characteristic of biomedical magnesium alloys [5]. The potential–time curves of the AZ63 samples in the simulated body fluid are displayed in Fig. 6. The typical potential–time curve of the untreated sample shows big changes indicative of dissolution and passivity of the magnesium alloy. With regard to sample 2, the free corrosion potential exhibits a sudden decrease at approximately 2200 s which corresponds to the active corrosion process [16]. The potential–time curve of sample 4 shows the reduced metastable localized corrosion nucleation phenomena after about 500 s, but rapid dissolution related to corrosion breakdown appears after about 3750 s. The free corrosion potential of sample 3 increases with longer immersion time and the presence of metastable pit nucleation with a lower frequency is indicated. The enhancement in the free corrosion potential means that a hybrid solution and aging treatment is beneficial to the initial stability of the alloy surface.

4. Discussion

As a bulk material, the phase constituents and their distribution as well as the grain size affect the corrosion properties significantly. AZ magnesium alloys are typically composed of a matrix of α grains with the β phase (the intermetallic $Mg_{17}Al_{12}$) along the α grain boundaries [17]. In a chloride solution, the corrosion performance of AZ alloy is determined by the β fraction, the continuous β phase around the α grains, and porosity. The amount and distribution of the β phase (discontinuous precipitation, DP and continuous precipitation, CP) determine the corrosion performance of the magnesium alloy. In particular, the β phase plays dual roles in the corrosion mechanism either as a corrosion barrier or galvanic cathode that accelerates corrosion. A homogeneously distributed β phase can more effectively retard corrosion, otherwise the presence of the β phase can accelerate corrosion [17]. It has been found that a solution or aged treatment can effectively change the distribution and amount of the β-$Mg_{17}Al_{12}$ phase [7].

Fig. 1 shows that the micro-structural evolution of the AZ63 alloy is accompanied by the redistribution of Al [8]. In comparison with the untreated sample 1, sample 2 possesses a more homogeneous surface morphology. The β phase dissolves in the α phase solid solution after a 24 h, 413 °C solution treatment followed by 1 h, 216 °C aging. Complete dissolution of the β phase leads to the formation of sharp grain boundaries and the structure of the secondary solidification region eventually evolves into the new well-defined α grains [7]. After 5.5 h aging, the DP and CP β phases appear gradually and with longer aging time, a large amount of the CP β phase forms inside the α grains. Compared to the RDC AZ91 alloy [7], a longer aging time is needed to form the precipitates of the β phase in the AZ63 alloy. It may be due to the lower aluminum content. The increase in the incubation period suggests depressed aging kinetics for the β phase in the AZ63 alloy.

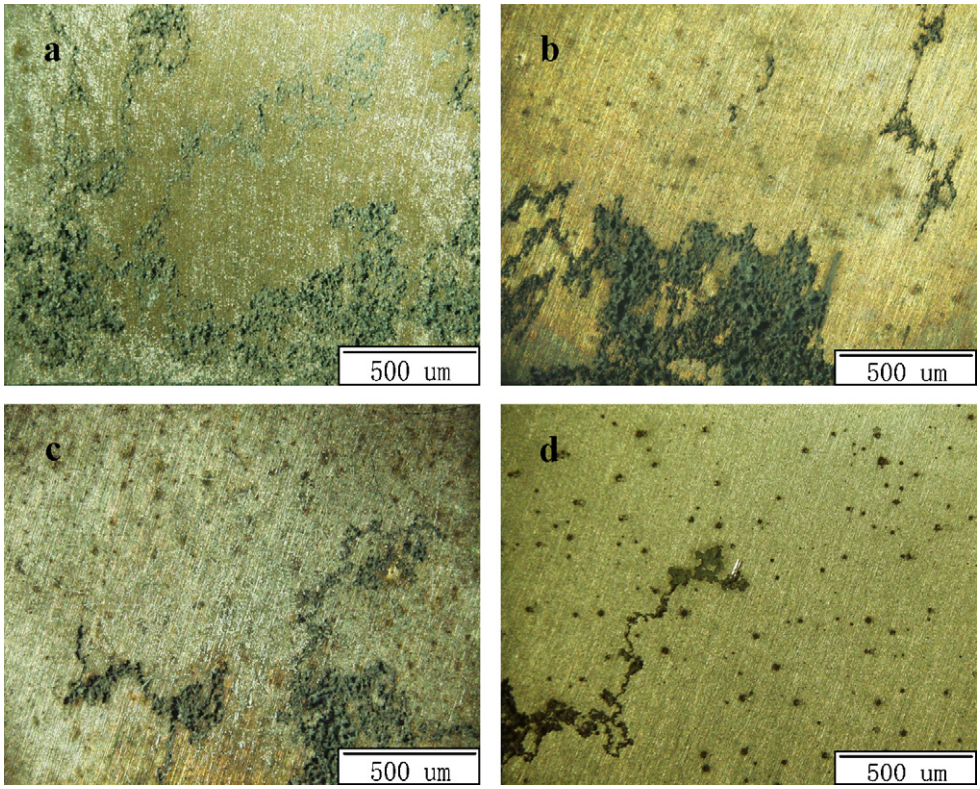

Fig. 5. Optical micrographs of the AZ63 surfaces after 14 days exposure in Tyrode's simulated body fluid for samples aged for different periods of time: (a) sample 1 (untreated), (b) 1 h, (c) 5.5 h, and (d) 12 h.

The in situ corrosion test results indicate that changes in the microstructure of the aged die-cast AZ63 Mg alloy have a great influence on the corrosion performance in the simulated body fluid. Although the surfaces of all the samples are polished by the same technique, different corrosion attack is observed for different immersion time. For sample 1 (untreated), uniform and deep corrosion take place. For the aged samples, filiform and pitting corrosion is shallow. After 12 h immersion, sample 1 shows more serious corrosion breakdown. Our results suggest that changes in the microstructure lead to the variations in the corrosion rates in the initial 12 h of exposure. Although the heat treatment alters the microstructure and redistributes the atoms, the initial corrosion breakdown takes place mainly at the centre of the α phase grain in all the treated samples, showing that the Al content is lower at the center of the α phase grain. The subsequent corrosion processes are different between the untreated and aged samples: uniform and deep corrosion on the untreated sample and filiform and pitting corrosion on the aged and treated samples. The typical micro-morphology of the filiform and shallow corrosion attack on the aged sample is shown in Fig. 7. It develops mainly along the center of the α phase grains.

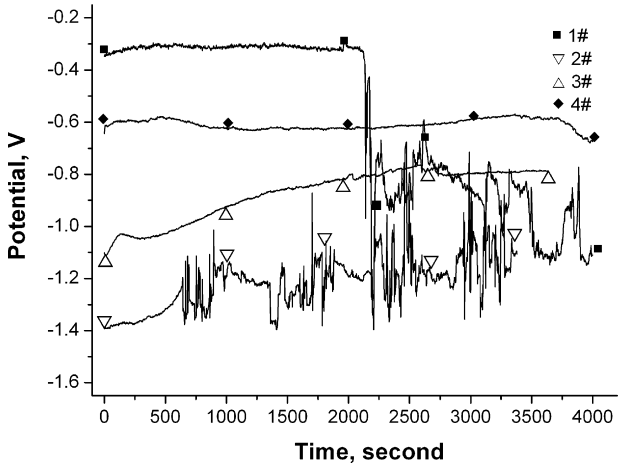

Fig. 6. Free corrosion potential–time curves acquired from AZ63 samples immersed in Tyrode's simulated body fluid.

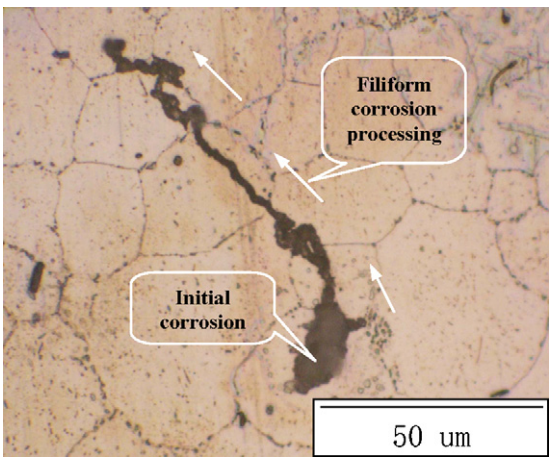

Fig. 7. Typical micro-morphology of the filiform corrosion on the aged and treated AZ63 alloy in Tyrode's simulated body fluid.

Some previous studies have pointed out that the volume fraction and distribution of the β phase have a large influence on the corrosion properties of AZ magnesium alloys [12,17,18]. Fig. 1a shows that the β phase is not abundant and its distribution is uneven. As a result, the inter-distance of the β phase can be very large thereby making interconnection almost impossible. Therefore, when corrosion commences from the center of the α phase grains, dissolution of the β phase is accelerated. That is to say, the β phase is a cathode to the α phase, and hydrogen evolution preferentially takes place from the β phase making it an effective cathode [18]. Daloz et al. [19] have pointed out that when the β phase fraction is large, the film formed on the β phase is more stable because of the presence of greater amount of aluminum that could act as a barrier to inhibit the dissolution of the α phase. Since the β phase fraction is low in the untreated AZ63 alloy, it is impossible to form a homogeneous protective film, and this is believed to be the main reason for the severe corrosion attack. In contrast, the aged AZ63 alloys have a more homogeneous microstructure (Fig. 1b–d) and more even distribution of aluminum. When exposed to air, the aluminum oxide formed over the α phase is more compact and uniform. A description of the formation of the oxide film outside the metallic surface consisting of $Mg(OH)_2$, MgO and Al_2O_3 has been proposed [11]. The existence of the Al_2O_3 layer may to a certain extent depress the capillary penetration of the test solution [20], thereby lengthening the degradation period in the simulated body fluid. The variation in the free corrosion potential measured from the untreated sample is extensive, indicating the usual behavior when subjected to a very high frequency of metastable pit nucleation [15]. In contrast, the free corrosion potentials of samples 3 and 4 continue to rise (Fig. 6) and it may be ascribed to the relatively compact and stable oxide film inhibiting capillary action of the test solution and blocking the corrosion attack. Compared to samples 3 and 4, a sudden decrease takes place at approximately 2200 s in the free corrosion potential for sample 1, indicating instability of the oxide film. After 14 days in the simulated body fluid, the surface morphologies of samples 3 and 4 are clearly different from those of the other two samples. The corrosion attack consists of not only filiform corrosion but also pitting corrosion. The appearance of pitting corrosion may be ascribed to the formation of the β phase. According to Fig. 1c and d, the β phase is formed along or inside the α phase grains. Moreover, the volume fraction of the β phase increases with longer aging time. It has been pointed out that a high volume fraction of the β phase that is also aluminum rich may mitigate the overall corrosion of the alloy [11–13]. Therefore, the existence of the β phase depresses the corrosion attack. Fig. 8 indicates the variation of the average corrosion rate for the different samples after 14 days immersion. The lowest corrosion rate is approximately 1/2 of that of the untreated sample. The change in the pH may also suppress the degradation rate of the AZ63 alloy in the simulated body fluid consisting of 0.9 wt.%NaCl. The dissolution of magnesium alloy in an aqueous solution with chloride ions proceeds by the following reactions.

$$Mg \rightarrow Mg^{2+} + 2e^-, \quad 2H_2O + 2e^- \rightarrow H_2 + 2(OH)^-,$$
$$Mg^{2+} + 2(OH)^- \rightarrow Mg(OH)_2 \qquad (2)$$

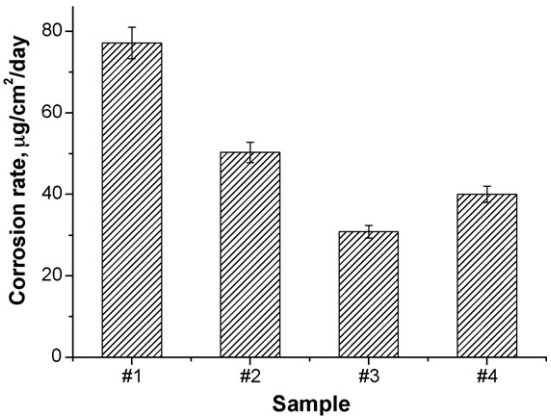

Fig. 8. Average corrosion rates of the untreated and aged AZ63 alloys after immersion in Tyrode's simulated body fluid for 14 days.

Altun et al. have shown that highly acidic solutions attack both magnesium and aluminum, and hence a very high corrosion rate and a pH value above ∼9 favor the formation of $Mg(OH)_2$ [21]. Chemically, both the forward and reverse reactions exist. Fig. 4b indicates that the pH value rises initially and then decreases after 48 h immersion. Before 48 h exposure, the release rate of magnesium ions rises almost exponentially. According to reaction (2), the great number of electrons raises the pH. Meanwhile, it can be determined that the forward reaction by which $Mg(OH)_2$ is formed may be promoted due to the higher pH. Because the $Mg(OH)_2$ film can inhibit corrosion of the magnesium alloy to some extent [4], the pH value decreases. At the same time, the chloride ions can transform $Mg(OH)_2$ to the more soluble $MgCl_2$ in order to attain the reaction balance, lots of $(OH)^-$ are needed to make $Mg(OH)_2$ causing re-dissolution of magnesium. At equilibrium, the pH only changes within a small range.

5. Conclusion

We have investigated the effects of heat treatment on the degradation of die-cast AZ63 Mg alloy in Tyrode's simulated body fluid. The solution treatment at 413 °C for 24 h followed by aging at 216 °C for up to 1 h leads to complete dissolution of the β phase into the α phase grains causing the formation of new well-defined α grains with sharp grain boundaries. The β-$Mg_{17}Al_2$ precipitates form after 5.5 h of aging, and the amount and distribution become greater and wider with longer aging time. With increasing aging time, the treated alloys show greater corrosion resistance. After 14 days immersion in 37 ± 1 °C Tyrode's simulated body fluid, the lowest corrosion rate achieved is about 1/2 of that of the untreated alloy. The change in the microstructure is thus shown to impact the corrosion behavior of the alloys. For the aged materials, shallow filiform and pitting corrosion is observed. In comparison, deep and uniform corrosion is observed on the untreated AZ63 alloy.

Acknowledgment

The project was supported by City University of Hong Kong Applied Research Grant (ARG) no. 9667002.

References

[1] A. Gefen, Med. Biol. Eng. Comput. 40 (2002) 311–319.
[2] X. Cao, M. Jahazi, J.P. Immarigeon, W. Wallace, J. Mater. Process. Technol. 171 (2006) 188–204.
[3] F. Witte, V. Kaese, H. Haferkamp, E. Switzer, H. Windhagen, Biomaterials 26 (2005) 3557–3563.
[4] G.L. Song, Adv. Eng. Mater. 7 (2005) 563–586.
[5] F. Witte, J. Fischer, J. Nellesen, H.A. Crostack, H. Windhagen, Biomaterials 27 (2006) 1013–1018.
[6] M. Wislawska, M. Janick-Czachr, Corros. J. 20 (1985) 36–45.
[7] Y. Wang, G. Liu, Z. Fan, Acta Mater. 54 (2006) 689–699.
[8] Z.Y. Zhang, X.Q. Zeng, W.J. Ding, Mater. Sci. Eng. A 392 (2005) 150–158.
[9] S. Mathieu, C. Rapin, J. Steinmetz, Corros. Sci. 45 (2003) 2741–2755.
[10] C. Scharf, A. Ditze, A. Shkurankov, E. Morales, K.U. Kainer, Adv. Eng. Mater. 7 (2005) 1134–1142.
[11] G.L. Song, A. Atrens, X.L. Wu, B. Zhang, Corros. Sci. 40 (1998) 1769–1791.
[12] T. Zhang, Y. Li, F.H. Wang, Corros. Sci. 48 (2006) 1249–1264.
[13] G.L. Song, A. Bowles, D. Stjohn, Mater. Sci. Eng. A 366 (2004) 74–86.
[14] M. Kuhlein, U. Galovsky, Mater. Corros. 55 (2004) 444–448.
[15] A. Fossati, F. Borgioli, E. Galvanetto, T. Bacci, Corros. Sci. 48 (2006) 1513–1527.
[16] J. Bolton, X. Hu, J. Mater. Sci. Mater. Med. 13 (2002) 567–574.
[17] G.L. Song, A. Atrens, M. Dargusch, Corros. Sci. 41 (1999) 249–273.
[18] R. Ambat, N.N. Aung, W. Zhou, Corros. Sci. 42 (2000) 1433–1455.
[19] D. Daloz, P. Steinmetz, G. Michot, Corrosion 83 (1997) 944–949.
[20] J. Masalski, J. Gluszek, J. Zabrzeski, P. Gluszek, Thin Solid Films 349 (1999) 186–190.
[21] H. Altun, S. Sen, Mater. Des. 25 (2004) 637–643.